Mater.Phys.Mech. 4 (2001) 17-21

A PRACTICAL NANOSCOPIC RAMAN IMAGING TECHNIQUE REALIZED BY NEAR-FIELD ENHANCEMENT

W.X. Sun and Z.X. Shen

Physics Department, Blk S12, Faculty of Science, National University of Singapore, 2 Science Drive 3, Singapore 117542

Received: July 3, 2001

Abstract. Near-field scanning optical microscope (NSOM) has the potential to become a very important tool for material characterization due to its ability to investigate the structure and micro-environment of materials in nano-scale by performing spectroscopy as well as topographic mapping. However, near-field Raman results have been rarely reported although Raman spectra are unique in chemical and structural identification. This is due to the fact that Raman signal is intrinsically weak (less than 1 in 10^7 photons) and the laser power emerging from tip is extremely low (typically 100 nW) because of the low optical throughput of metal coated fiber tips. The long integration time (typically 10 minutes per spectrum) required for collecting good quality Raman spectra makes it impractical to construct a Raman image through this conventional method. In this paper, we report an integration of NSOM and Raman spectrometer using an apertureless configuration, in which the laser is focused onto the sample through a microscope objective and Raman signal is collected by the same objective. This is similar to the conventional micro-Raman except that a metal tip is brought into the laser spot on sample surface to enhance the Raman signal through surface enhanced Raman scattering (SERS). Raman enhancement of 10^4 times has been achieved and Raman mapping on real silicon devices has been realized with 1 second exposure time. Furthermore, the reflection scattering geometry employed in our experiments allows the study of any sample without specific sample preparation, unlike the conventional SERS which needs coating samples with metal or growing sample on metal surface.

1. INTRODUCTION

Raman spectroscopy measures molecular vibrations, which are determined by the structure and chemical bonding as well as the masses of the constituent atoms/ions. Raman (like infrared) spectra are unique in chemical and structural identification. Conventional (far-field) micro-Raman spectroscopy has a spatial resolution of about 0.5 μm, governed by the theoretical diffraction limit, while the IR spectrometer has a best spatial resolution of about 10 μm due to its longer wavelength. Near-field scanning Raman microscopy (NSRM) is based on the principle of near-field scanning optical microscopy (NSOM): an optical fiber tip with a small aperture (50-100 nm) is used to deliver the laser light and the fiber tip is kept at a close constant distance (~ tens nanometer) above the sample surface. Raman signal is collected in far field through either microscope objective or a lens [1-3]. The laser spot size on the sample is defined by the tip aperture (near-field) in this case and an NSOM image is formed by scanning the fiber tip across the sample surface. In NSRM, the scattered light is coupled to a Raman spectrometer where Raman spectra are recorded for each point on the sample. An NSRM image is constructed using these spectra.

Although NSOM is still not a mature technique, NSOM and NSOM-fluorescence have been extensively used, especially in the study of biological systems [4-6], semiconductor [7,8] and thin films [9,10]. On the other hand, NSRM has not found widespread application despite its uniqueness in providing structural/chemical specific information and nanometer spatial resolution. The main reason for this is that Raman signal is intrinsically week (less than 1 in 10^7 photons) and the very low laser power emerging from the fiber tip (typically 100 nW). A typical

Corresponding author: Z.X. Shen, e-mail: physzx@nus.edu.sg

Raman spectrum takes about several minutes to collect using the conventional fibre tip NSRM method, making it prohibitive to construct a Raman image this way. The Raman images (no more than 30 by 30) reported in references [1,3] took more than 9 hours to obtain the data. Although extensive efforts have been devoted to fabricate fiber tips with larger laser output [11-13], the throughput is still quite low, especially for the tips with an aperture less than 200 nm.

An alternative approach to the optical fiber tips is to use apertureless metal tips, employing surface enhanced Raman scattering (SERS) which can improve the Raman intensity by several orders of magnitude [14,15]. In this case, the Raman enhancement is a result of local field enhancement by the metal tip, which is either due to the enhancement of the electromagnetic field in the vicinity of sharply pointed tip or due to the excitation of surface plasma by the laser electromagnetic wave, or increased polarizability of the sample due to the interaction between the tip and sample. The apertureless NSRM has been used to record Raman images in transmission mode [16].

In this paper, we report the near-field Raman mapping of a real Si device using the reflection mode. Using the apertureless approach, we have developed an NSRM system by integrating an NSOM microscope and a Raman spectrometer. The key feature of our NSRM system is that we constructed our instrument using the reflection geometry. While the transmission NSRM can only be applied to transparent and very thin samples, which are very restrictive for applications, our method can apply to any samples in principle which is a giant step forward towards real applications of NSRM. The main drawback of our approach is the unwanted far-field Raman signal collected together with the near-field signal. The near-field signal has to be comparable to the far-field signal in order to obtain good quality Raman images. In our experiments, the near-field enhancement factor is estimated to be more than 10^4 times and a good quality Raman spectrum can be collected with less than 1 s integration time using modest laser power. We have successfully obtained 1-D Raman mapping of a real Si device with 1 s exposure time, and there is no obstacle in principle to collect 2D Raman images. This is a very significant development in NSRM as it is the first demonstration that this technique can be used for imaging purpose because of the short integration time. Another crucial important advantage of our approach in comparison with other SERS is that the enhancement is achieved using the metal tip rather than by coating the sample with Ag as normally done in SERS experiments. This means that our method will be applicable to ANY sample and no sample preparation is needed, making it an extremely powerful analytical technique for both fundamental research and applications.

2. INSTRUMENTATION

The NSRM system used in our experiments consists of a standard Nanonics NSOM system and a Renishaw Raman spectrometer. The NSOM is controlled by a Burleigh controller and the control software can control the Renishaw spectrometer through Dynamic Data Exchange. The system can acquire AFM and Raman spectra simultaneously. Nanonics NSOM uses bent tips, which allow the easy integration of the spectrometer and Nanonics NSOM by putting the scanning head under the microscope objective (Nikon, X50, WD 13.8 mm and NA 0.45) of the Renishaw system, as shown in Fig. 1. An argon laser (488 nm line) is focused onto the metal tip. In our experimental configuration, the tip apex is not shadowed, as the laser beam is a focused beam with a converging angle of 26.7°, while the half angle of the tip is only about 4°. In addition, the tip is not perpendicular to sample surface where the angle between the tip axis and sample surface is about 60°.

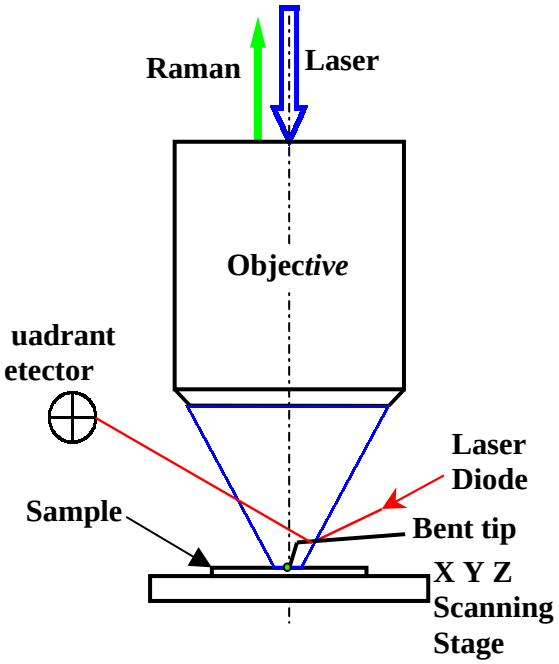

Fig. 1. Schematic Diagram of Apertureless NSOM-Raman in backscattering geometry.

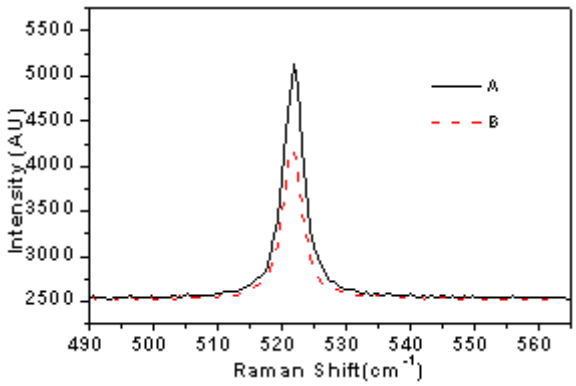

Fig. 2. The silicon Raman spectra with the tip "touching" the sample surface (spectrum A) and the tip withdrawn (spectrum B).

The interaction between the tip and the laser enhances the local electrical field near the tip, which in turn enhances the Raman signal nearby. The same objective collects the Raman signal in laser spot in the backscattering geometry, which includes both the far-field and near-field Raman signal, which are coupled into the spectrometer by coupling optics. During a scan, the tip is fixed relative to the laser spot while the sample runs a raster scan.

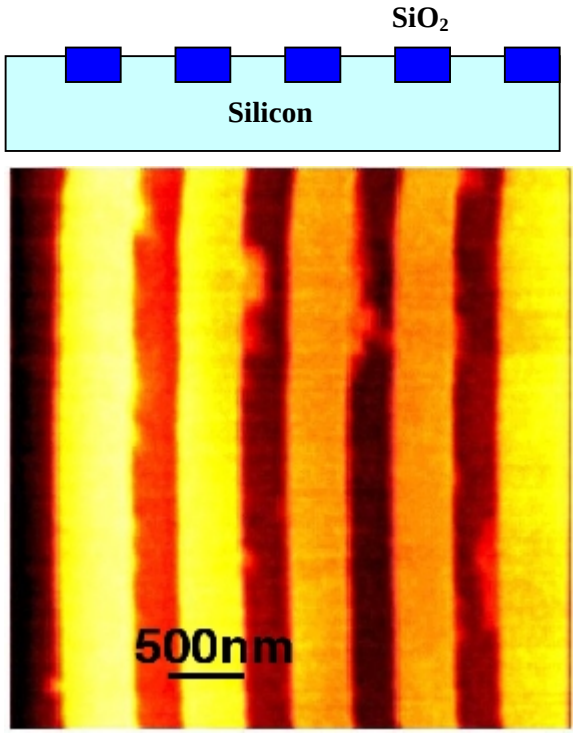

Fig. 3. a) Schematic cross-sectional diagram of the Si device sample; b) AFM image of the Si device sample. The image was acquired by the NSOM with a metal tip used in this experiment.

3. EXPERIMENTAL RESULTS

To demonstrate the capability of our NSRM system, we have carried out two types of experiments on Si samples. The first experiment was performed on a pure Si single crystal to show near-field enhancement and the second experiment was mapping of a Si device to show the spatial resolution of NSRM. In the first experiment, a blank silicon wafer was placed on the piezo scanning stage of the NSOM system and the silicon Raman peak at 520 cm^{-1} was recorded by Raman spectrometer for two tip positions: (1) the tip "touching" the silicon surface to record the Raman spectrum which includes both the near-filed and far-field components, and (2) the tip lifted about 100 μm from the surface to record the far-field Raman spectrum. Spectra A & B in Fig. 2 show, respectively, the Raman spectra recorded under the two situations above. The near-field component consists about 35 % of the total signal in spectrum A. The enhancement factor of the near-field Raman signal can be estimated as follows. In our experimental set-up, the laser spot size is about 3 μm in diameter and the penetration depth of the 488 nm laser into the Si sample is about 0.5 μm. Assuming that the diameter of the metal tip is 100 nm and the near-field enhancement occurs at a depth of 20 nm of the Si sample. The far-field signal comes from a volume of $_{far} = \pi(3000/2)^2 \times 500\,\mathrm{nm}^3$, while the near-field signal comes from a much smaller volume $_{near} = \pi(100/2)^2 \times 20\,\mathrm{nm}^3$. The enhancement factor can be estimated as $\frac{I_{near}}{I_{far}} \times \frac{V_{far}}{V_{near}} = 12115$, where $I_{near} = 0.35I$ and $I_{far} = (1-0.35)I$ are the measured near and far field Raman intensity respectively. This factor is in the same order as the calculated near-field enhancement using the generalized field propagator method [17].

In the second experiment, we performed Raman mapping using the NSRM system to show the improved spatial resolution with the apertureless tip. Fig. 3a shows schematically the cross section of a silicon device sample and Fig. 3b is an AFM image of the sample. The width of the silicon lines is 300 nm, and the SiO_2 lines are 380 nm in width, 350 nm in depth and 30 nm higher than the silicon lines. In the NSRM experiment, a total of 128 Raman spectra were recorded with 1 second integration time across the lines. The Raman intensity, peak width and frequency at each point on the device were derived by fitting the spectra with Gaussian profile using

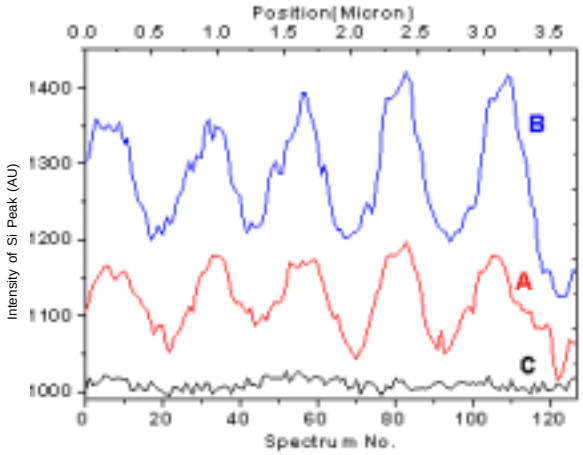

Fig. 4. Raman mapping of the Si device sample across the Si lines. Curves A and B are generated from two sets of Raman spectra acquired using two different metal tips. Curve C is generated from far-field Raman spectra.

an Array Basic program developed by us. In Fig. 4, we plot the Raman intensity of Si against the serial number of the Raman spectra that corresponds to different positions on the device shown in Fig. 3b, e.g. Number 1 and 128 are the left most and right most points respectively. The two curves A and B shown in Fig. 4 are two Raman mappings of the same Si lines with different tips, showing good reproducibility of this method. We have also collected Raman mapping of the same Si lines using the micro-Raman setting, i.e. with the tip lifted and the Raman intensity does not show any variation with position, as shown in Fig. 4C.

Note that the far-field component of the Si Raman peak comes from the whole illuminated region (3 μm) which is much bigger than the size of the Si or SiO_2 lines. Hence the far-field Raman intensity is independent of the position on the Si device as demonstrated by the featureless micro-Raman mapping mentioned above. On the other hand, the near-field component comes from a small region (~100 nm) near the tip only, which will show variation with the position on the device. Hence the Raman intensity variation shown in Fig. 4 is a clear manifestation of near-field enhancement while the far-field Raman contributes a constant background. Stronger Raman intensity was obtained when the tip was on silicon lines, corresponding to the valleys in the AFM, and weaker Raman intensity on SiO_2 lines. This can be readily understood that the near-field component is strong when the tip in on Si, while it is absent when the tip is on SiO_2 as the SiO_2 is too thick to allow any near-field enhancement of the Si peak.

4. CONCLUSION

An apertureless near-field Raman microscope was realized in the reflection geometry by integrating a NSOM and a Raman spectrometer in this paper. The apertureless configuration is a breakthrough to the limitation set by the low optical throughput of metal coated optical fiber tips, therefore reduces the integration time for Raman spectrum drastically. The reflection scattering geometry makes the system applicable to any samples without preparation. Hence the reflection NSRM has great potential in Raman nanoscopy and imaging.

REFERENCES

[1] S. Webster, D.A. Smith and D.N. Batchelder // *Vibrat. Spectrosc.* **18** (1998) 51.
[2] E. J. Ayars and H.D. Hallen // *Appl. Phys. Lett.* **76** (2000) 3911.
[3] C.L. Jahncke, M.A. Paesler and H.D. Hallen // *Appl. Phys. Lett.* **67** (1995) 2483.
[4] Lewis, A. Radko, N. B. Ami, D. Palanker and K. Lieberman // *Trends in Cell Biology* **9** (1999) 70.
[5] Th. Enderle, T. Ha, D.S. Chemla and S. Weiss // *Ultramicroscopy* **71** (1998) 303.
[6] E. Monson, G. Merritt, S. Smith, J.P. Langmore and R. Kopelman // *Ultramicroscopy* **57** (1995) 257.
[7] Y. Toda, S. Shinomori, K. Suzuki and Y. Arakawa // *Appl. Phys. Lett.* **73** (1998) 517.
[8] G. Wurtz, R. Bachelot and P. Royer // *Eur. Phys. J. AP* **5** (1999) 269.
[9] P. F. Barbara, D.M. Adams and D.B. O'Connor // *Annu. Rev. Mater. Sci.* **29** (1999) 433.
[10] J. C. Conboy, E. J. C. Olson, D. M. Adams, J. Kerimo, A. Zaban, B. A. Gregg and P. F. Barbara // *J. Phys. Chem. B* **102** (1998) 4516.
[11] M. N. Islam, X. K. Zhao, A. A. Said, S. S. Mickel and C. F. Vail // *Appl. Phys. Lett.* **71** (1997) 2886.
[12] T. Yatsui, M. Kourogi and M. Ohtsu // *Appl. Phys. Lett.* **73** (1998) 2090.
[13] Y. H. Chuang, K. G. Sun, C. J. Wang, J. Y. Huang and C. L. Pan Rev. // *Rev. Sci. Instrum.* **69** (1998) 437.
[14] M. Kerker, D. S. Wang and H. Chew // *Appl. Opt.* **19** (1980) 3373.
[15] F. Adrian // *Chem. Phys. Lett.* **78** (1981) 45.

[16] R. M. Stöckle, Y. D. Suh, V. Deckert and R. Zenobi // *Chem. Phys. Lett.* **318** (2000) 131.

[17] O.J.F. Martin, C. Girard and A. Dereux // *Phys. Rev. Lett.* **74** (1995) 526 .